Theoretical Studies on Pyridoxal 5′-Phosphate-Dependent Transamination of α-Amino Acids

RONG-ZHEN LIAO, WAN-JIAN DING, JIAN-GUO YU, WEI-HAI FANG, RUO-ZHUANG LIU
College of Chemistry, Beijing Normal University, Beijing 100875, People's Republic of China

Received 29 July 2007; Revised 15 January 2008; Accepted 16 January 2008
DOI 10.1002/jcc.20958
Published online 25 March 2008 in Wiley InterScience (www.interscience.wiley.com).

Abstract: Density functional methods have been applied to investigate the irreversible transamination between glyoxylic acid and pyridoxamine analog and the catalytic mechanism for the critical [1,3] proton transfer step in aspartate aminotransferase (AATase). The results indicate that the catalytic effect of pyridoxal 5′-phosphate (PLP) may be attributed to its ability to stabilize related transition states through structural resonance. Additionally, the PLP hydroxyl group and the carboxylic group of the amino acid can shuttle proton, thereby lowering the barrier. The rate-limiting step is the tautomeric conversion of the aldimine to ketimine by [1,3] proton transfer, with a barrier of 36.3 kcal/mol in water solvent. A quantum chemical model consisting 142 atoms was constructed based on the crystal structure of the native AATase complex with the product L-glutamate. The electron-withdrawing stabilization by various residues, involving Arg386, Tyr225, Asp222, Asn194, and peptide backbone, enhances the carbon acidity of 4′-C of PLP and Cα of amino acid. The calculations support the proposed proton transfer mechanism in which Lys258 acts as a base to shuttle a proton from the 4′-C of PLP to Cα of amino acid. The first step (proton transfer from 4′-C to lysine) is shown to be the rate-limiting step. Furthermore, we provided an explanation for the reversibility and specificity of the transamination in AATase.

 J Comput Chem 29: 1919–1929, 2008

Key words: pyridoxal 5′-phosphate; transamination; proton-transfer; aspartate aminotransferase; density functional theory

Introduction

Pyridoxal 5′-phosphate (PLP)[1–10] is ubiquitous and central to a wide variety of anabolic and catabolic pathways in the metabolism of amino acids. Aspartate aminotransferase (AATase) is one of the most extensively studied PLP dependent enzymes, catalyzing the reversible interconversion of dicarboxylic amino and keto acids[11–13] (Scheme 1). PLP acts as a coenzyme, alternating between keto and amine forms in the two half-reactions that constitute a catalytic cycle.

Based on the crystallographic studies and numerous kinetic, spectroscopic, and mutational studies, the following reaction mechanism (Scheme 2) has emerged for Aspartate aminotransferase.[14–20] PLP forms a Schiff base with the ε-amino group of Lys258, with a pK_a relatively lower than the usual PLP Schiff base in aqueous solutions and existing equilibrium between the protonated and unprotonated forms. The Michaelis complex is rapidly converted to the external aldimine via transimination. Proton abstraction from C_α of the substrate by Lys258 produces the quinonoid intermediate and reprotonation at 4′-C of PLP gives the ketimine which yields keto acid and E•PMP (enzyme-bound pyridoxamine 5′-phosphate) after hydrolysis. However, from hydrogen kinetic isotope effects a concerted [1,3] proton transfer mechanism was proposed for cytoplasmic isozyme of AATase with L-aspartate whereas a stepwise mechanism for mitochondrial AATase with L-glutamate.[21] Furthermore, ^{13}C and ^{15}N kinetic isotope effects suggested the contribution of Cα—H cleavage, ketimine hydrolysis, and oxaloacetate dissociation to the rate limitation.[22] In the second half of the reaction, another α-keto acid reacts with PMP to yield a new L-amino acid. The enantiospecificity of the product is of ongoing focus[23–28] due to the biological requirement for L-transamination in constituting L-amino acids.

This article contains supplementary material available via the Internet at http://www.interscience.wiley.com/jpages/0192-8651/suppmat.

Correspondence to: J. -G. Yu; e-mail: jianguo_yu@bnu.edu.cn

Contract/grant sponsor: National Natural Science Foundation of China; contract/grant numbers: 20573011, 20403003

Contract/grant sponsor: Major State Basic Research Development Programs; contract/grant numbers: 2004CB719903, 2002CB613406

Scheme 1

Experimental researches have shown that transamination reactions with PLP as a co-factor can be simulated by heating a mixture of an appropriate amino acid and stoichiometric equivalent of pyridoxal.[29–38] Pyridoxal was found to be converted to pyridoxamine and the reaction was fully reversible with the exception of glycine and pyridoxal.[30] The transamination could only occur between pyridoxamine and glyoxylic acid to yield pyridoxal and glycine. However, it is still unknown how an α-substituent influences the reaction equilibrium. Established kinetic studies on the reaction of pyridoxal and selected amino acids suggested that the [1,3] proton transfer is the rate-limiting step.[39,40] On account of the unique reactivity of PLP and PMP in biological systems, many attempts have been made to develop biomimetic compounds using these cofactors, particularly for transamination reaction.[41–51]

Quantum chemical computational method has been used to study the reactivity of PLP in decarboxylation,[52,53] 1,2-amino mutation,[54] Schiff base formation,[55,56] transimination,[57,58] and racemization.[59–61] However, as far as we know, there are few established theoretical works directed to the understanding of the proton-transfer, where the inclusion of PLP plays an important role in determining the chirality of newly formed amino acid in enzymatic transamination. Salvà et al.[56] have performed DFT calculations on the Schiff base formation of 3-hydroxy-4′-pyridinaldehyde, methylamine, and one water molecule, which shows that the dehydration is the rate-determining step. In our previous study,[62] we found the carboxylic group is indispensable in the transamination reaction as it results in an alternate mechanism through general acid-catalysis.

In the last 10 years, many researchers have applied quantum chemical methods to study the enzymatic reaction mechanism using a relatively small model of enzyme active site.[63–68] The rest of the enzyme is usually considered as a homogenous polarizable medium and can normally be treated by dielectric cavity techniques. With the computer power of today, using DFT method, one is able to handle system up to 100 atoms. Generally, it is necessary to employ as small models as possible of the active site, in order to limit the computational time. At the same time, one has to choose the quantum chemical model carefully in order to reproduce the chemistry that occurs in the enzyme active site to such a high degree that it can be used as polestar to answer mechanistic and energetic questions. This methodology has been applied for many enzymes, often with great success.[63–68]

In this article, the reactivity of pyridoxamine in respect to transamination with glyoxylic acid was studied by DFT calculations. The calculated results provide a detailed energetic profile for transamination, in good agreement with the experimental result,[39,40] in which the tautomeric conversion of ketimine to

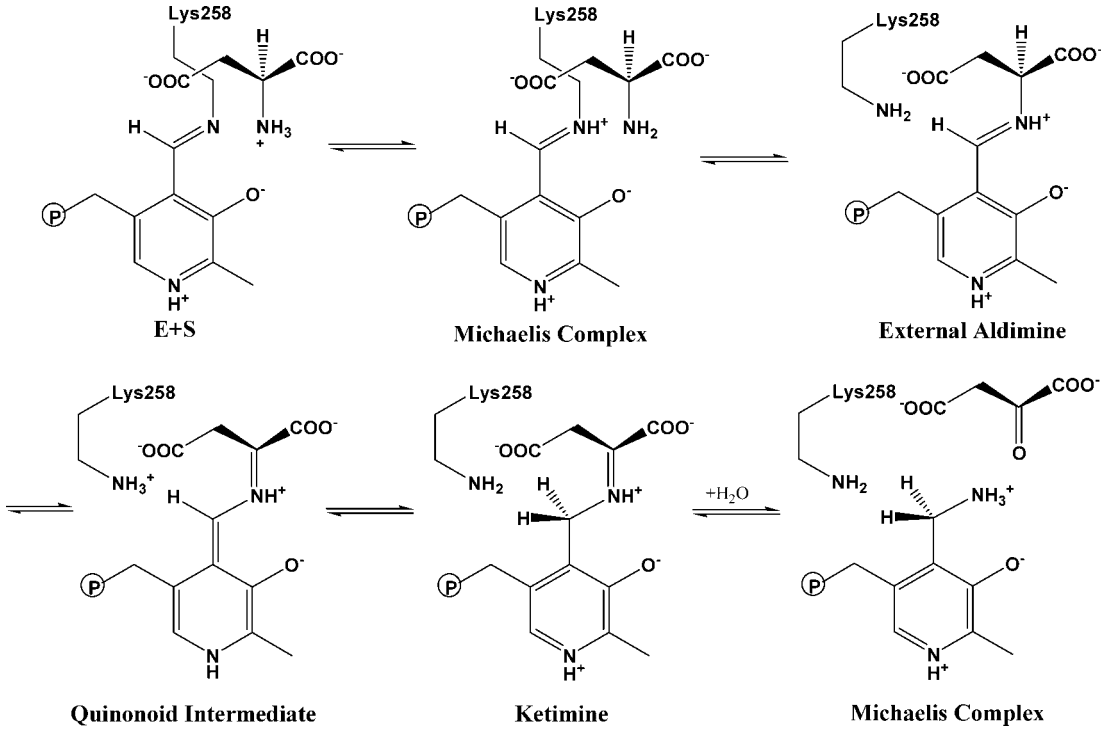

Scheme 2. Reaction mechanism of Aspartate aminotransferase with L-aspartate.

aldimine is rate-limiting. This also provides an opportunity to compare with the direct transamination in order to ascertain the catalytic effect of PLP. In addition, the proton transfer steps catalyzed by Aspartate aminotransferase with L-glutamate is investigated with a large quantum chemical model of the active site constructed based on the crystal structure of the enzyme complex with L-glutamate.[69] The aim is to shed more light on the reaction mechanism and specificity of AATase.

Computational Details

The molecular complex consisting of a pyridoxamine analog and glyoxylic acid was used to simulate the transamination reaction. Theoretical calculations presented herein were carried out using the Gaussian98 and Gaussian03 program packages.[70,71] The geometries of reactants, products, intermediates, and transition states involved in this reaction have been fully optimized at the B3LYP[72,73] level of theory. The 6-31G(*d,p*) basis sets were used for the small model, while the 6-31G(*d*) basis sets were used for the large model and additional p-type polarization function was added for the transferred hydrogen atom [labeled as 6-31G(d)*]. Single-point calculations were performed with the 6-311++G(*2df,2pd*) basis sets on the optimized geometries for model reaction while the 6-311+G(*2d,2p*) basis set was used to correct the basis set effect for the large enzyme active site model. The identity of all critical points was confirmed by analytical frequency calculations and structures were characterized as residing at first-order saddle points (transition states, or TS for short) or minima (equilibrium geometries) on the potential energy hypersurfaces. Selected reaction pathways were subjected to intrinsic reaction coordinate (IRC)[74,75] analyses, in order to trace their paths and to confirm that the optimized TS structures connect the corresponding two structures residing at minima. In the enzyme model, fixing the truncation atoms to their crystallographically observed positions gave rise to a few small negative eigenvalues. These are very small, in the order of -10 cm^{-1}, and do not affect the obtained energetic results. In addition, the entropic contributions can not be estimated properly and were thus omitted. The solvation effect of water has been considered by B3LYP/6-311++G(2*df,2pd*) single point calculations on the B3LYP/6-31G(*d,p*) optimized gas-phase geometries using a relatively simple self consistent reaction field (SCRF)[76] model using the UAHF set of solvation radii to build the cavity for the solute in the gas-phase, which is based on the polarizable continuum model (PCM) of the Tomasi's group.[77–79] For the large active site model, the energetic effects of the protein environment were estimated by solvation with a dielectric constant (ε) chosen to be 4 calculated at the B3LYP/6-31G(*d*)* level, which is the standard value used in modeling protein surroundings.[80] When the quantum chemical model of the active site is selected properly, the selection of dielectric constant changes the energetics slightly (less than 2 kcal/mol), as a large active site model already contains at the quantum level most of the polarization around the reactive center of the active site (see Results and Discussion section below). Usually, when large solvent effects are obtained, it is indicative of some deficiencies in the chemical model of the active site. The final energies reported below are obtained from the large basis set calculations, corrected for zero point vibrational energies and solvation effects.

Results and Discussion

In this study, the full mechanism for the transamination between pyridoxamine analog and glyoxylic acid was investigated in gas phase first, then with water solvation correction. Unlike the current gas phase model, the pyridine nitrogen might be protonated and the carboxylate deprotonated. It should be noted that it is not easy to simulate all the real processes for transamination in water solution using quantum chemical approach. The only reliable model would be to include water cluster interacting with the reactive center directly, which should also be treated at high level in order to describe the interactions properly. However, such kind of calculations is hardly feasible and determining the accurate kinetic information for transamination in water solution is beyond the scope of this article. Our present approach still provides reliable qualitative and quantitative results related to the intrinsic properties of these two molecules. The whole process may be divided into five main steps (Scheme 3), similar to those in our previous study[62] on a direct transamination: carbinolamine formation, dehydration, [1,3] proton transfer, hydrolysis, and carbinolamine elimination. The optimized structures of reactant complex (Re), all transition states, and product complex (Pr) are sketched in Figure 1, whereas the structures of all intermediates are shown in the supporting information. The detailed discussion of the mechanism and the calculated energetics (Fig. 2) is presented in the following subsections.

Carbinolamine Formation

In our calculations, reactant complex Re (Fig. 1) was taken as the initial structure of this reactive process, in which N9 of PLP is located nearly perpendicular to the glyoxylic acid plane with a dihedral angle of -96.2°, formed by atoms 9, 10, 12, 11, and at a distance of 2.570 Å from C10. O13 forms a hydrogen bond with H15 at the distance of 1.858 Å. Because of the hydrogen bonding interactions, the energy of Re is 3.9 kcal/mol (see Table 1) lower than that of isolated reactants in the gas phase.

The nucleophilic attack is performed via TS1 (Fig. 1), in which the distance of C10–N9 is 1.647 Å. The barrier is calculated to be 7.7 (-0.6) kcal/mol (energies in parenthesis correspond to calculations including water solvation effect) relative to Re. Downhill from TS1, a zwitterionic intermediate Int1 is formed with a proton transfer from O14 to O12. In Int1, the key distance of C10-N9 is 1.547 Å, and N9 bears a positive charge while the carboxylic group is anionic. Int1 is relatively unstable, and can produce the carbinolamine Int2 through TS2 (Fig. 1) in which H15 is transferred from O7 to O13 and at the same time H11 is transferred from N9 to O7. TS2 has been confirmed to be a first-order saddle point with an imaginary frequency of 608i cm^{-1}. The barrier for TS2 is calculated to be barrierless (-0.9 kcal/mol relative to Int1). This is due to the including zero-point vibrational energy, which would lower the barrier (by 2.3 kcal/

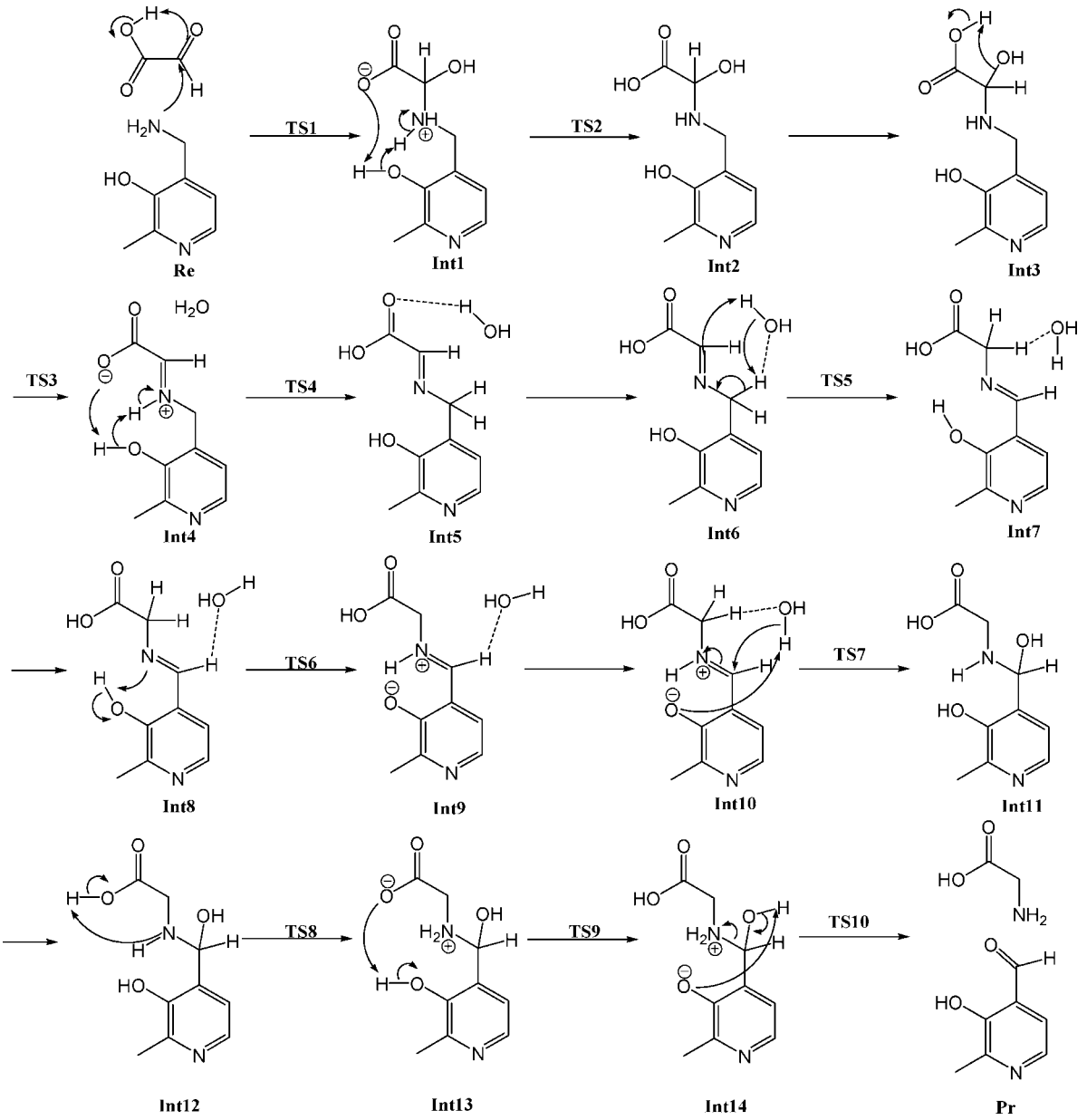

Scheme 3. Suggested mechanism for transamination between pyridoxamine and glyoxylic acid from calculations.

mol for TS2) especially for transition states involving proton transfer, as the classical electronic energy barrier is slightly positive (+1.4 kcal/mol). This kind of phenomena has also been found in barrier calculations on low barrier hydrogen bond and water cluster neutral-zwitterionic tautomerization.[81–83] However, it can be confirmed that this step is very fast. The hydroxyl group of the PLP acts as a proton transferring carrier, thereby lowering the barrier.

Because of the adjacent carboxylic group being a proton donor, the carbinolamine is formed through a stepwise mechanism with a barrier even lower than that in Salvà's one water assisted but lacking a carboxylic group model.[56] Including water solvent effect, the carbinolamine will be formed without barrier according to our calculations. The schematic potential energy surface is shown in Figure 2.

Dehydration

The Schiff base formation involves eliminating a water molecule from the carbinolamine moiety. In the current model, Int2 need to isomerize to Int3 through two single bond rotation. Then the dehydration occurs through a five-centered ring transition state TS3 in which a proton has already transferred from the carboxylic group to the hydroxyl group. After

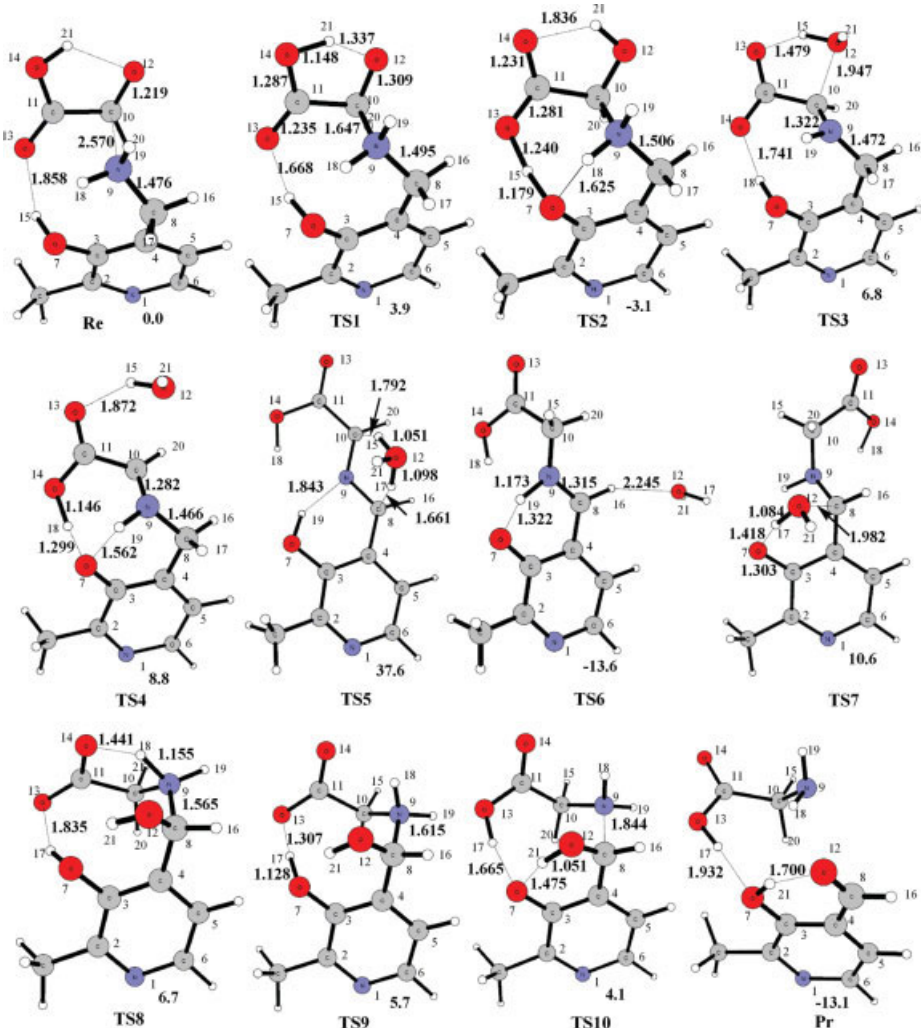

Figure 1. Structures of the reactant complex, transition states, product complex for the transamination between pyridoxamine analog and glyoxylic acid with geometry optimized at the B3LYP/6-31G(d,p) level. Selected inter-atomic distances are given in angstroms. The relative energy for each structure is also listed (in kcal/mol).

TS3, a zwitterionic imine Int4 is formed, which would regenerate a neutral imine Int5 through a concerted proton transfer transition state TS4 in which H19 transfers from N9 to O_7 whereas H_{18} is transferring from O7 to O14. In the first step, the carboxylic group participates in the dehydration by deprotonation whereas the PLP hydroxyl group stabilizes it, whereas in the second step, the PLP hydroxyl group acts as a proton transfer bridge. The results show that the barriers for these two steps are 16.9 (8.9) and 18.8 (16.6) kcal/mol relative to Int3. However, PLP is not as good as water in lowering the barrier as our previous study has shown that the barriers for these two steps with one water molecule assisted are 13.4 kcal/mol and 5.9 kcal/mol.[62] Comparing the barriers of the carbinolamine formation and dehydration (see Fig. 2), we can see that the latter step is the rate-limiting step in the Schiff base formation, which is in good agreement with experimental kinetic studies.[84–88]

[1,3] Proton Transfer

The tautomeric conversion of ketimine to aldimine requires a [1,3] proton transfer. If H17 is replaced by a methyl group or some others, this proton transfer would produce a chiral amino acid. However, in non-enzymatic transamination reaction both L and L configurations are formed with zero specific rotation as both H16 and H17 can be transferred without stereo-selectivity. The pK_a of α-H is 29 for zwitterionic glycine,[89] while it decreases to 17 for a glycine pyridoxal Schiff base,[90] indicating a much easier α-deprotonation process. However, the energetic cost will be still very high.

In the current model, the water molecule produced from the dehydration step was used to assist this step. In Int5, the water molecule is hydrogen bonded to the carboxylic group, in order to assist the proton transfer, it has to be hydrogen bonded to H_{17} with the formation of Int6. A twisted six-centered ring transition

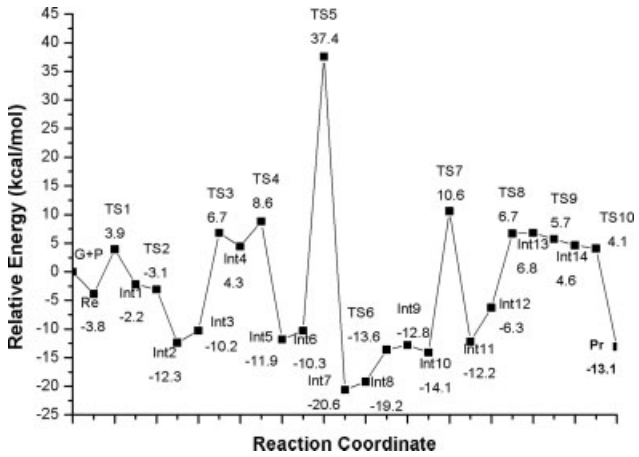

Figure 2. Reaction profiles for the transamination of glyoxylic acid and pyridoxamine analog in gas-phase calculated at the B3LYP/6-311++G(2df,2pd)//B3LYP/6-31G(d,p) level.

state TS5 (Fig. 1) was located, the structure of which corresponds to a situation in which the hydrogen from CH_2 is being transferred to the water molecule, which, in turn, has already started to transfer hydrogen to C10 in a concerted way. Not surprisingly, this transition state corresponds to the highest energy barrier of the reaction path. From Int6 to TS5, C4-C8 decreases from 1.516 Å to 1.467 Å, which might allow structural resonance between the anionic carbon and pyridine ring. However, there is no change of electron density (less than 0.01e) of the pyridoxyl ring from Int6 to TS5, which have also been found in theoretical studies on PLP dependent decarboxylation.[52] It does not appear to be driven by the accepted paradigm of electron delocalization through "electron sink". It is found that the phenolic OH forms stronger hydrogen bond with the reactive nitrogen (H—N distance of 1.843 Å) in TS5 than that (1.993 Å) in Int6. The barrier is 47.7 (33.4) kcal/mol relative to Int6 that is about 7 kcal/mol lower than that in direct transamination between glycine and formaldehyde in our previous study.[62] This is in consistent with the fact that the pK_a of α-C in glycine is lowered when bounded to pyridoxal. The high barrier indicates that water is not a good bridge to assist the [1,3] proton transfer, although adding more water molecules might lower the barrier somewhat. In solution, the [1,3] proton transfer might be assisted by an acid or a base, thereby lowering the barrier. From the data in Table 1, it can be seen that the newly formed aldimine Int7 is 10.3 (9.0) kcal/mol more stable than ketimine due to the conjugation effect in the former, while the reverse reaction is hard to occur, which can explain the experimental result that no transamination occur between pyridoxal and glycine. The reason for the equilibrium transamination between pyridoxal plus alanine and pyridoxal plus pyruvic acid may be the compromise of the hindrance between methyl and carboxylic group in aldimine and the conjugation effect.

Schiff Base Hydration

The hydrolysis of aldimine is the addition of one water molecule to the newly formed C=N double bond. First, Int7 isomerizes to Int8 in which the water molecule is hydrogen bonded to H16 with a distance of 2.245 Å. From Int8, H19 connected to O7 is transferred to N9 through TS6 that makes C8 more electrophilic, the resulting zwitterionic intermediate Int9 lies 6.4 (2.1) kcal/mol higher than Int8. This kind of zwitterionic structure has also been located for the Schiff base formed by pyridoxal and alanine, which lies 1.5 kcal/mol higher than the corresponding neutral form at MP2/6-31G(d) level.[52] Then Int9, with the water molecule hydrogen bonded to H_{16}, isomerizes to Int10 with the water molecule hydrogen bonded with the carboxylic group, this intermediate was located from the IRC calculation of the next water addition transition state. From Int10, the water molecule attacks C8 at the same time H17 transferred to O7 through a twisted six-centered transition state TS7. In TS7, the distances of O12-O8, H17-O7 are 1.982 Å, 1.418 Å, respectively. This step is calculated to be the rate-limiting step for hydrolysis, with an accumulated barrier of 31.2 (19.2) kcal/mol relative to Int7. Unlike the dehydration step, the carboxylic group has little influence on the hydrolysis as it is far away from the reactive center, instead, the PLP hydroxyl group participates in the water addition by acting as a proton donor and acceptor.

Carbinolamine Elimination

The transamination is accomplished with the elimination of the newly formed carbinolamine to yield pyridoxal and glycine. The carbinolamine Int11 produced from the hydrolysis cannot be eliminated directly, unless it isomerizes to Int12 through three single bond revolutions which can occur easily and will not be discussed here. The mechanism for elimination can be seen as zwitterionic and stepwise. First, H18 from the carboxylic group is transferred to N9 through TS8 (see Fig. 1) and forms a zwitterionic intermediate Int13, in which N9 is the positive center

Table 1. Relative Energies (in kcal/mol) for the Stationary Points Along the Transamination Path, Computed at the B3LYP/6-311++G(2df,2pd)//B3LYP/6-31G(d,p) Level of Theory.

	Relative energies			Relative energies	
	Gas-phase	SCRF-PCM (water)		Gas-phase	SCRF-PCM (water)
G + P	0.0	0.0	Int8	−19.2	−15.9
Re	−3.8	1.9	TS6	−13.6	−12.3
TS1	3.9	1.3	Int9	−12.8	−12.8
Int1	−2.2	−8.5	Int10	−14.1	−11.1
TS2	−3.1	−9.0	TS7	10.6	3.5
Int2	−12.3	−9.6	Int11	−12.2	−15.2
Int3	−10.3	−7.7	Int12	−6.3	−4.7
TS3	6.7	1.2	TS8	6.7	1.0
Int4	4.3	−0.3	Int13	6.8	−2.7
TS4	8.6	8.9	TS9	5.7	−5.1
Int5	−11.9	−6.7	Int14	4.6	−3.2
Int6	−10.3	−6.7	TS10	4.1	−1.1
TS5	37.4	26.7	Pr	−13.1	−8.8
Int7	−20.6	−15.7			

Table 2. Detailed Description of the AATase Active Site Mode Used in the Current Calculations.

	Part included from crystal structure	Possible role in the model	Fixed positions
PLP	Whole part with phosphate excluded	Covalent bond with substrate	Oxygen bound to Phosphate and 2′-C
Lys258	Propanamine	Shuttling proton	C_γ
Arg386	*N*-methyl-guanidine	Binding substrate and electrostatic stabilization	C_δ
Arg292b	*N*-methyl-guanidine	Binding substrate	C_δ
Asp222	Acetic acid	Locking PLP	C_β
His143	Methyl-imidazole	Hydrogen bonding with Asp222	C_β
Tyr70b	Phenol	Hydrogen bonding with Lys258	C_γ
Tyr225	Phenol	Hydrogen bonding with pheonic oxygen of PLP	C_γ
Asn194	Acetamide	Hydrogen bonding with Arg386 and pheonic oxygen of PLP	C_β
Ile37–Gly38–Val39	*N*-formyl-glycine amide	Hydrogen bonding with α-carboxylate and Lys258	Backbone C(Ile37) and N(Val39)

and the carboxylate is the negative one. This proton-transfer weakens the C—N bond with its elongation to 1.600 Å. Then H17 is transferred from O7 to the carboxylate through TS9 (see Fig. 1) and makes the negative center transferred to O7. At the end, C8-N9 is elongated and H21 is transferred to O7 through TS10 to yield the product Pr. The participation of hydroxyl group and carboxylic group of PLP lowers the barrier of proton transfer. From Figure 2 it can be seen that the elimination step occurs with lower barrier than the hydrolysis.

Proton Transfer in Aspartate Aminotransferase

The model cluster used to simulate the active site of AATase was built starting from the 2.4 Å X-ray structure of *E. coli* AATase in complex with L-glutamic acid (PDB code 1X28).[69] The coenzyme PLP forms a Schiff base with the substrate glutamate, which is locked by Arg386 and Arg292b (b indicates residues from another chain), in addition, Asp222 interacts with N1 of PLP. The proposed catalytic base Lys258 is located in the si-face.[91,92] All these parts are included in the quantum chemical model. Additionally, all other important residues form hydrogen bonds with the above reactive center are included, such as Ile37-Gly38-Val39 peptide backbone, Tyr70b, His143, Asn194, and Tyr225. Trp140, involved in π-stacking with PLP ring and hydrogen bonding with substrate side chain carboxylate, is not included as it would have a small effect on delocalizing the negative charge from the PLP ring during the proton transfer. It should be noted that the phosphate group has been omitted on the ground that it should not have a big effect upon the electron distribution of the reactive center. Although this negative charged fragment, which interacts with Arg266 and two additional peptide chains (Ser255–Phe256–Ser257 and Gly107–Gly108–Thr109), could exert a Coulombic influence on the reactive center and fix Tyr70b through hydrogen bond, these effects should be relatively small as there is no direct resonance interaction with the pyridoxal ring and lysine, and the interactions with all stationary points along the reaction path would be almost the same. The different parts of the model, their possible role, and points of truncation are shown in Table 2. The optimized geometry of the reactant species is shown in Figure 3. Lys258 is neutral, as in the native enzyme, the nearby positively charged Arg386 and Arg292b will lower the pK_a of Lys258 much. Experimentalists also proposed an equilibrium between a protonated form and a non-protonated form.[69] However, only a neutral Lys258 will be reactive to act as the proposed base to catalyze the proton transfer. Asterisks(*) show atoms which are kept frozen at their crystallographically observed positions. This kind of strategy can keep the various groups with their locations as much as possible resembling the crystal structure. If done properly, this technique will ensure the structural integrity of the model, but still with enough flexibility. The final quantum chemical model is composed of 142 atoms and has an overall charge of zero.

We started with a structure of Asp222 deprotonated by pyridine nitrogen, however, an automatic proton transfer was observed during the optimization, this might be an artifact of current gas phase model. The protonation state should have

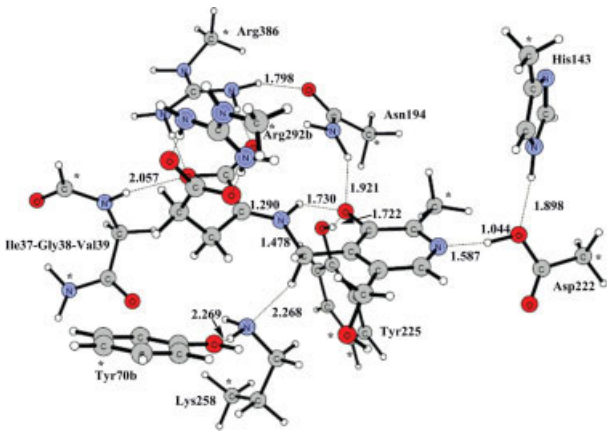

Figure 3. Optimized structure of the AATase active site with a substrate molecule 2-oxoglutarate (AA-Re). Distances are in angstroms. [Color figure can be viewed in the online issue, which is available at www.interscience.wiley.com.]

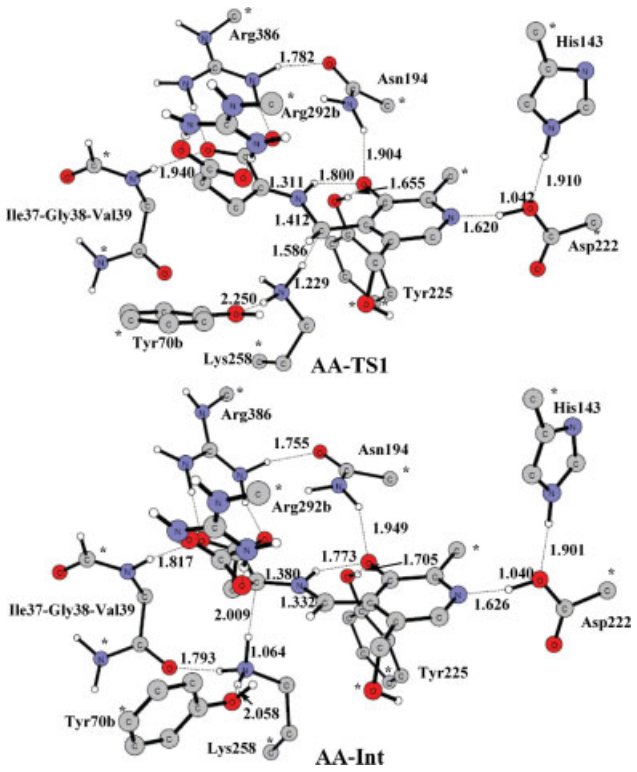

Figure 4. Optimized structures for the first proton transfer transition state (AA-TS1) and resulting intermediate (AA-Int). Distances are in angstroms.

some influence on the barrier of the [1,3] proton transfer, however, as will be discussed below, this effect is relatively small. The first step of the suggested AATase reaction mechanism is the proton transfer from 4′-CH_2 of PLP to ε-N of Lys258. In AA-Re, The ε-N in Lys258 is in a perfect position to accept a proton from PLP, with a distance of 2.268 Å. The transition state for the first step (AA-TS1) was located, and the optimized AA-TS1 structure and the resulting intermediate structure AA-Int are shown in Figure 4. In AA-TS1, the key C-H and N-H distances are 1.586 and 1.229 Å, respectively. Without including the solvation effects, the barrier is 19.1 kcal/mol and AA-Int lies 10.3 kcal/mol higher than AA-Re.

To approximately estimate the energetic effects of the parts of the enzyme that is not included in the quantum chemical model, the surrounding is assumed to be a homogenous polarizable medium with some dielectric constant ε. In the current study, $\varepsilon = 4$ and $\varepsilon = 80$ was used to investigate the influence of dielectric constants on the energetics. As seen in Figure 5, the barrier is changed less than 0.5 kcal/mol from $\varepsilon = 4$ (19.6 kcal/mol) to $\varepsilon = 80$ (19.9 kcal/mol).

The second step is the proton transfer back from Lys258 to α-C of oxoglutarate. We have optimized the transition state (AA-TS2, shown in Figure 6) for this step. This step occurs with a barrier of 1.4 kcal/mol relative to AA-Int (10.2 kcal/mol relative to AA-Re) in gas phase. However, when including the solvation effect, it will occur with a slightly negative barrier

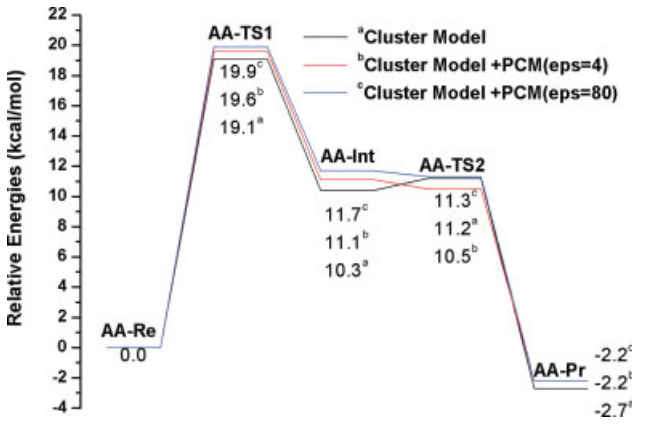

Figure 5. Potential energy profile for the proton transfer with 2-oxoglutarate as a substrate in AATase.

(−0.6 kcal/mol relative to AA-Int). At AA-TS2 (see Fig. 5), the critical distance between proton and α-C of oxoglutarate is 1.532 Å, whereas the distance between proton and ε-N of Lys258 is 1.250 Å. The tautomerization is slightly exothermic, with a value of 2.7 kcal/mol in gas phase (2.2 kcal/mol with solvation

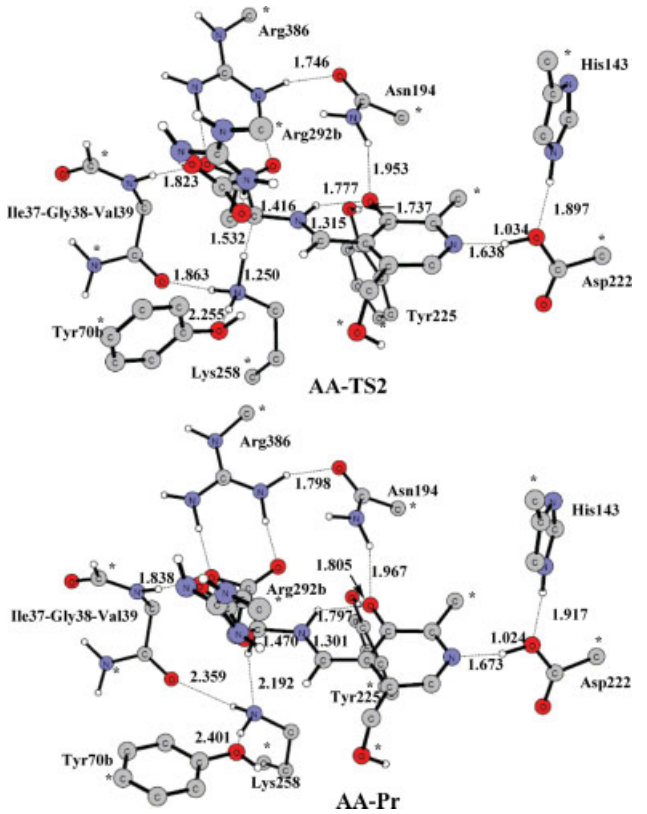

Figure 6. Optimized structures for the second proton transfer transition state (AA-TS2) and resulting product (AA-Pr). Distances are in angstroms.

correction), consistent with the experimental observed reversible transamination in AATase.

Experimental rate constants for the transamination in AATase from different organisms with oxoglutarate are found to be in the range of 100–600 s^{-1},[93–95] which can be transformed into barriers of around 14–16 kcal/mol by using classical transition state theory. In our calculations, the rate-limiting step for the [1,3] proton transfer is the proton transfer from 4′-CH_2 of PLP to ε-N of Lys253, with a barrier of 19.6 kcal/mol, about 3-5 kcal/mol higher than the experimental ones. There may be several reasons for this barrier overestimation. First, the proton transfer from Asp222 to Pyridine nitrogen should lower the barrier slightly as it can stabilize the transition state more than the reactant. We fixed the critical N—H distance at 1.0 Å and optimized the corresponding structures for AA-Re, AA-Int1, and AA-Pr (these proton transferred structures labeled as AA-Re-pt, AA-Int-pt, AA-Pr-pt and shown in supporting information). In gas phase, AA-Re-pt lies 5.1 kcal/mol higher than AA-Re, in addition, AA-Int-pt and AA-Pr-pt are 6.1 and 0.8 kcal/mol relative to AA-Re-pt, respectively. As AA-Int has the largest charge separation between Lys258 and PLP, AA-Int has 2.7 kcal/mol additional stabilization energy from this proton transfer. (AA-Int lies 8.8 kcal/mol higher than AA-Re without including the ZPE, the stabilization energy was derived from large basis set calculations.) It is reasonable to predict that when the pyridine nitrogen is protonated by Asp222, the barrier may be lowered by around 2 kcal/mol or even less. Previous theoretical calculations on PLP dependent decarboxylation also found that this proton transfer has small influence on the barrier.[52] Although the reaction type is different, the role of this proton transfer is the same in both cases. Second, the role of Tyr70b is to stabilize the positive Lys258 during the proton transfer, however, the hydrogen bond distance between Tyr70b and Lys258 becomes just 0.019 Å shorter from AA-Re to AA-TS1, the transition stabilization seems to be underestimated. The reason might be the truncation of Tyr70b at C_γ, including one more carbon atom might lower the barrier slightly. Third, the computational method (in this case DFT B3LYP functional and the employed basis sets) can not be ruled out as a possible source of error. In addition, the entropy effect is not included as it can not be calculated accurately due to the fixing of atoms. However, these changes are not of such a magnitude that they will alter any conclusion about the mechanism of AATase.

In AATase, Lys258 is the catalytic base, the proton transfer introduces protonated Lys258, Tyr70b, and Ile37-Gly38-Val39 peptide backbone to stabilize it through hydrogen bonding. At the same time, the heterolytic cleavage of C—H results in the negative charge delocalization at the PLP plane, while Tyr225, Arg386, and Ile37-Gly38-Val39 peptide backbone interact with PLP plane through hydrogen bonds, the corresponding distances are all shorter in AA-TS1 than those in AA-Re, as shown in Figures 3 and 4.

From the crystal data in the PDB, it can be seen that all the L-transaminases have the catalytic lysine residue in the si-face whereas all the D-transaminases have a lysine in the re-face.[91,92] The position of catalytic base lysine determines the stereospecificity of newly formed amino acid. Furthermore, our calculations also provide an explanation of why D-amino acids are not reactive. First, Arg292b and Arg286 lock the two carboxylate group of aspartate, the D-amino acids will not bind well as its α-H is in the si-face of PLP. Second, there is no appropriate base in the si-face, the only possibility to allow [1,3] proton transfer is to use a water solvent molecule to assist this step on the assumption that it is water accessible. However, as we discussed before, the barrier for a water assisted [1,3] proton transfer is over 40 kcal/mol in gas phase, thus this side-reaction would not compensate with the natural one even with the stabilization of residues around the active site. Unlike amino acid racemase, there is no amino acid like Tyrosine in the re-face to protonate Cα,[60,61] therefore no racemization would occur in AATase. Furthermore, decarboxylation, another important class of biochemical reactions involving α-amino acids, cannot yet occur because of the salt bridge between the α-carboxylate and Arg386, which makes the decarboxylation have a very high barrier due largely to the separation of charge.[52]

Conclusions

A theoretical examination of the detailed mechanism of PLP dependent transamination was reported in this article. For the transamination between pyridoxamine and glyoxylic acid, our results indicate that the proton-transfer between ketimine and aldimine is the rate-limiting step with the barrier of 36.3 kcal/mol in water solution. In this system the aldimine is much more stable than the ketimine, which could explain the irreversibility for such specific transamination. The carboxylic group and the PLP hydroxyl group play an important role in the reaction by shuttling a proton. We also investigated the enzymatic proton transfer in AATase using a large quantum chemical model. It was found that Lys258 acts as a general base to shuttle the proton from 4′-C of PLP to α-C of amino acid, providing strong evidence for the mechanism proposed experimentally. We were also able to provide an explanation for the experimentally observed specificity and reversibility of AATase. The role of different residues in the active site was analyzed. Interestingly, the protonation of pyridine nitrogen by Asp222 does not lower the barrier much.

References

1. Lichstein, H. C.; Gunsalus, I. C.; Umbreit, W. W. J Biol Chem 1945, 161, 311.
2. Green, D. E.; Leloir, L. F.; Nocito, V. J Biol Chem 1945, 161, 559.
3. O'kane, D. E.; Gunsalus, I. C. J Biol Chem 1947, 170, 425.
4. Meister, A. Science 1954, 120, 43.
5. Karpeisky, M. Y.; Ivanov, V. I. Nature 1966, 210, 493.
6. Evangelopoulos, A. E.; Sizer, I. W. Proc Natl Acad Sci USA 1963, 49, 638.
7. Morino, Y.; Snell, E. E. Proc Natl Acad Sci USA 1967, 57, 1692.
8. Walsh, C. In Enzymatic Reaction Mechanisms, Freeman: San Francisco, 1979, p. 777.
9. Ford, G. C.; Eichele, G.; Jansonius, J. N. Proc Natl Acad Sci USA 1980, 77, 2559.

10. Eliot, A. C.; Kirsch, J. F. Annu Rev Biochem 2004, 73, 383.
11. Christen, P.; Metzler, D.E. Transaminases, New York: Wiley, 1985.
12. Kiick, D. M.; Cook, P. F. Biochemistry 1983, 22, 375.
13. Kirsch, J. F.; Eichele, G.; Ford, G. C.; Vicent, M. G.; Jansonius, J. N.; Gehring, H.; Christen, P. J Mol Biol 1984, 74, 497.
14. McPhalen, C. A.; Vinvent, M. G.; Picot, D.; Jansonius, J. K.; Lesk, A. M.; Chothia, C. J Mol Biol 1992, 227, 197.
15. Jäger, J.; Moser, M.; Sauder, U.; Jansonius, J. N. J Mol Biol 1994, 239, 285.
16. Rhee, S.; Silva, M. M.; Hyde, C. C.; Rogers, P. H.; Metzler, C. M.; Metzler, D. E.; Arnone, A. J Biol Chem 1997, 272, 17292.
17. Okamoto, A.; Higuchi, T.; Hirotsu, K.; Kuramitsu, S.; Kagamiyama, H. J Biochem 1994, 116, 95.
18. Toney, M. D.; Kirsch, J. F. Biochemistry 1993, 32, 1471.
19. Hayashi, H.; Mizuguchi, H.; Kagamiyama, H. Biochemistry 1998, 37, 15076.
20. Park, Y.; Luo, L.; Schultz, P. G.; Kirsch, J. F. Biochemistry 1997, 36, 10517.
21. Julin, D. A.; Kirsch, J. F. Biochemistry 1989, 28, 3825.
22. Rishavy, M. A.; Cleland, W. W. Biochemistry 2000, 39, 7546.
23. Ayling, J. E.; Dunathan, H. C.; Snell, E. E. Biochemistry 1968, 7, 4537.
24. Vederas, J. C.; Floss, H. G. Acc Chem Res 1980, 13, 455.
25. Yoshimura, T.; Nishimura, K.; Ito, J.; Esaki, N.; Kagamiyama, H.; Manning, J. M.; Soda, K. J Am Chem Soc 1993, 115, 3897.
26. Nishimura, K.; Ito, J.; Yoshimura, T.; Esaki, N. Soda, K. Bioorg Med Chem 1994, 2, 605.
27. Jhee, K.-H.; Yoshimura, T.; Esaki, N. Soda, K. Biochemistry, 1996, 35, 9792.
28. Shin, J.-S.; Kim, B. -G. J Org Chem 2002, 67, 2848.
29. Snell, E. E. J Am Chem Soc 1945, 67, 194.
30. Snell, E. E.; Metzler, D. E. J Am Chem Soc 1952, 74, 979.
31. Metzler, D. E.; Olivard, J.; Snell, E. E. J Am Chem Soc 1954, 76, 644.
32. Metzler, D. E.; Ikawa, M.; Snell, E. E. J Am Chem Soc 1954, 76, 648.
33. Cennamo, C.; Carafoli, B.; Bonetti, E. P. J Am Chem Soc 1956, 78, 3523.
34. Matsuo, Y. J Am Chem Soc 2016, 1957, 79.
35. Bruice, T. C.; Topping, R. M. J Am Chem Soc 1962, 84, 2448.
36. Blake, M. I.; Siegel, F. P.; Katz, J. J.; Kilpatrick, M. J Am Chem Soc 1963, 85, 294.
37. Shigenobu, M.; Yoshikazu, M. J Am Chem Soc 1972, 94, 7211.
38. Bruno, S.; Martell, A. E. Inorg Chem 1986, 25, 327.
39. Banks, B. E. C.; Dianantis, A. A.; Vernon, C. A. J Chem Soc 1961, 4235.
40. Pishchugin, F. V.; Tuleberdiev, I. T. Russuan. J Gen Chem 2005, 75, 1538.
41. Breslow, R.; Hammond, M.; Lauer, M. J Am Chem Soc 1980, 102, 421.
42. Zimmerman, S. C.; Czarnik, A. W.; Breslow, R. J Am Chem Soc 1983, 105, 1694.
43. Winkler, J.; Coutouli-Argyropoulou, E.; Leppkes, R.; Breslow, R. J Am Chem Soc 1983, 105, 7198.
44. Czarnik, A. W.; Breslow, R. Carbohyd Res 1984, 128, 133.
45. Zimmerman, S. C.; Breslow, R. J Am Chem Soc 1984, 106, 1490.
46. Chmielewski, J.; Breslow, R. Heterocycles 1987, 25, 533.
47. Breslow, R.; Chmielewski, J.; Foley, D.; Johnson, B.; Kumabe, N.; Varney, M.; Mehra, R. Tetrahedron 1988, 44, 5515.
48. Breslow, R.; Canary, J. W.; Varney, M.; Waddell, S. T.; Yang, D. J Am Chem Soc 1990, 112, 5212.
49. Fasella, E.; Dong, S. D.; Breslow, R. Bioorgan Med Chem 1999, 7, 709.
50. Svenson, J.; Zheng, N.; Nicholls, I. A. J Am Chem Soc 2004, 126, 8554.
51. Liu, L.; Zhou, W. J.; Chruma, J.; Breslow, R. J Am Chem Soc 2004, 126, 8136.
52. Bach, R. D.; Canepa, C.; Glukhovtsev, M. N. J Am Chem Soc 1999, 121, 6542.
53. Toney, M. D. Biochemistry, 2001, 40, 1378.
54. Wetmore, S. D.; Smith, D. M.; Radom, L. J Am Chem Soc 2001, 123, 8678.
55. Salvà, A.; Donoso, J.; Frau, J.; Muñoz, F. J Mol Struct:THEOCHEM 2002, 577, 229.
56. Salvà, A.; Donoso, J.; Frau, J.; Muñoz, F. J Phys Chem A, 2003, 107, 9409.
57. Salvà, A.; Donoso, J.; Frau, J.; Muñoz, F. Int J Quantum Chem 2002, 89, 48.
58. Salvà, A.; Donoso, J.; Frau, J.; Muñoz, F. J Phys Chem A 2004, 108, 11709.
59. Ondrechen, M. J.; Briggs, J. M.; McCammon, J. A. J Am Chem Soc 2001, 123, 2830.
60. Major, D. T.; Nam, K.; Gao, J. J Am Chem Soc 2006, 128, 8114.
61. Major, D. T.; Gao, J. J Am Chem Soc 2006, 128, 16345.
62. Liao, R. -Z.; Ding, W. -J.; Yu, J. -G.; Fang, W. -H.; Liu, R. -Z. J Phys Chem A, 2007, 111, 3184.
63. Siegbahn, P. E. M. J Comput Chem 2001, 22, 1634.
64. Himo, F.; Siegbahn, P. E. M. Chem Rev 2003, 103, 2421.
65. Noodleman, L.; Lovell T.; Han, W. -G.; Li, J.; Himo, F. Chem Rev 2004, 104, 459.
66. Siegbahn, P. E. M.; Borowski, T. Acc Chem Res 2006, 39, 729.
67. Himo, F. Theo Chem Acc 2006, 116, 232.
68. Leopoldini, M.; Russo, N.; Toscano, M. J Am Chem Soc 2007, 129, 7776.
69. Islam, M. M.; Goto, M.; Miyahara, I.; Ikushiro, H.; Hirotsu, K.; Hayashi, H. Biochemistry 2005, 44, 8218.
70. Frisch, M. J.; Trucks, G. W.; Schlegel, H. B.; Scuseria, G. E.; Robb, M. A.; Cheeseman, J. R.; Zakrzewski, V. G.; Montgomery, J. A., Jr.; Stratmann, R. E.; Burant, J. C.; Dapprich, S.; Millan, J. M.; Daniels, A. D.; Kudin, K. N.; Strain, M. C.; Farkas, O.; Tomasi, J.; Barone, V.; Cossi, M.; Cammi, R.; Mennucci, B.; Pomelli, C.; Adamo, C.; Clifford, S.; Ochterski, J.; Petersson, G. A.; Ayala, P. Y.; Cui, Q.; Morokuma, K.; Malick, D. K.; Rabuck, A. D.; Raghavachari, K.; Foresman, J. B.; Cioslowski, J.; Ortiz, J. V.; Stefanov, B. B.; Liu, G.; Liashenko, A.; Piskorz, P.; Komaromi, I.; Gomperts, R.; Martin, R. L.; Fox, D. J.; Keith, T.; Al-Laham, M. A.; Peng, C. Y.; Nanayakkara, A.; Gonzalez, C.; Challacombe, M.; Gill, P. M. W.; Johnson, B.; Chen, W.; Wong, M. W.; Andres, J. L.; Head-Gordon, M.; Replogle, E. S.; Pople, J. A.; Gaussian 98; Gaussian Inc.: Pittsburgh, PA, 1998.
71. Frisch, M. J.; Trucks, G. W.; Schlegel, H. B.; Scuseria, G. E.; Robb, M. A.; Cheeseman, J. R.; Montgomery, J. A.; Vreven, T., Jr.; Kudin, K. N.; Burant, J. C.; Millam, J. M.; Iyengar, S. S.; Tomasi, J.; Barone, V.; Mennucci, B.; Cossi, M.; Scalmani, G.; Rega, N.; Petersson, G. A.; Nakatsuji, H.; Hada, M.; Ehara, M.; Toyota, K.; Fukuda, R.; Hasegawa, J.; Ishida, M.; Nakajima, T.; Honda, Y.; Kitao, O.; Nakai, H.; Klene, M.; Li, X.; Knox, J. E.; Hratchian, H. P.; Cross, J. B.; Adamo, C.; Jaramillo, J.; Gomperts, R.; Stratmann, R. E.; Yazyev, O.; Austin, A. J.; Cammi, R.; Pomelli, C.; Ochterski, J. W.; Ayala, P. Y.; Morokuma, K.; Voth, G. A.; Salvador, P.; Dannenberg, J. J.; Zakrzewski, V. G.; Dapprich, S.; Daniels, A. D.; Strain, M. C.; Farkas, O.; Malick, D. K.; Rabuck, A. D.; Raghavachari, K.; Foresman, J. B.; Ortiz, J. V.; Cui, Q.; Baboul, A. G.; Clifford, S.; Cioslowski, J.; Stefanov, B. B.; Liu, G.; Liashenko, A.; Piskorz, P.; Komaromi, I.; Martin, R. L.; Fox, D. J.; Keith, T.; Al-Laham, M. A.; Peng, C. Y.; Nanayakkara, A.; Challacombe, M.; Gill, P. M. W.; John-

son, B.; Chen, W.; Wong, M. W.; Gonzalez, C.; Pople, J. A. GAUSSIAN03, Revision B. 02; Gaussian Inc.: Pittsburgh, PA, 2003.
72. Becke, A. D. J Chem Phys 1993, 98, 5648.
73. Lee, C.; Yang, W.; Parr, R. G. Phys Rev B 1988, 37, 785.
74. Gonzalez, C. Schlegel, H. B. J Chem Phys 1989, 90, 2154.
75. Gonzalez, C. Schlegel, H. B. J Phys Chem 1990, 94, 5523.
76. Tomasi, J.; Persico, M. Chem Rev 1994, 94, 2027.
77. Cances, E.; Mennucci, B.; Tomasi, J. J Chem Phys 1997, 107, 3032.
78. Cossi, M.; Barone, V.; Cammi, R.; Tomasi, J. Chem Phys Lett 1996, 255, 327.
79. Barone, V.; Cossi, M.; Tomasi, J. J Comput Chem 1998, 19, 404.
80. Blomberg, M. R. A.; Siegbahn, P. E. M.; Babcock, G. T. J Am Chem Soc 1998, 120, 8812.
81. Garcia-Viloca, M.; González-Lafont, A.; Lluch, J. M. J Phys Chem A, 1997, 101, 3880.
82. Garcia-Viloca, M.; González-Lafont, A.; Lluch, J. M. J Am Chem Soc 1997, 119, 1081.
83. Anick, D. J. J Phys Chem A, 2003, 107, 1348.
84. Matsushima, Y. Chem Pharm Bull 1968, 16, 2151.
85. Sayer, J. M.; Pinsky, B.; Schonbrunn, A; Washtien, W. J Am Chem Soc 1974, 96, 7998.
86. Sayer, J. M.; Jenks, W. P. J Am Chem Soc 1977, 99, 464.
87. Sayer, J. M.; Conlin, P. J Am Chem Soc 1980, 102, 3592.
88. Echevarría, G. R.; Santos, J. G.; Basagoitia, A.; Blanco, F. G. J Phys Org Chem 2005, 18, 546.
89. Rios, A.; Crugeiras, J.; Amyes, T. L.; Richard, J. P. J Am Chem Soc 2001, 123, 7949.
90. Toth, K. Richard, J. P. J Am Chem Soc 2007, 129, 3013.
91. Kochhar, S.; Christen, P. Eur J Biochemistry, 1992, 203, 563.
92. Soda, K.; Yoshimura, T.; Esaki, N. Chem Rec 2001, 1, 373.
93. Wilkie, S. E.; Warren, M. J Protein Exp Purif 1998, 12, 381.
94. Campos-Cavieres, M.; Munn, E. A. Biochem J 1973, 135, 683.
95. Nobe, Y.; Kawaguchi, S.; Ura, H.; Nakai, T.; Hirotsu, K.; Kato, R.; Kuramitsu, S. J Biol Chem 1998, 273, 29554.